J Mater Sci (2023) 58:1694–1707

Energy materials

Highly flexible cellulose-based hydrogel electrolytes: preparation and application in quasi solid-state supercapacitors with high specific capacitance

Pingxiu Zhang[1], Meng Li[1], Yidan Jing[1,*], Xiaomin Zhang[1,*], Shengpei Su[1], Jin Zhu[2], and Ningya Yu[1,*]

[1] National and Local Joint Engineering Lab for New Petro-chemical Materials and Fine Utilization of Resources, Hunan Normal University, Changsha 410081, People's Republic of China

[2] Key Laboratory of Bio-based Polymeric Materials, Ningbo Institute of Material Technology and Engineering, Chinese Academy of Sciences, Ningbo 315201, People's Republic of China

Received: 21 September 2022
Accepted: 20 December 2022
Published online: 4 January 2023

ABSTRACT

Cellulose has received extensive attention as hydrogel electrolytes in energy storage fields, due to its renewable and environmentally friendly properties. However, it is still difficult to prepare cellulose-based hydrogel electrolytes for supercapacitors with high flexibility, high specific capacitance, and good temperature resistance. Herein, a series of cellulose-based hydrogel electrolytes with good mechanical properties were prepared successfully by incorporating with a small amount of acrylamide/*N*, *N*′-methylene bisacrylamide via a simple one-pot strategy and, successively, the resultant hydrogel electrolytes were assembled with the commercial activated carbon, as electrode materials, yielding quasi solid-state symmetric supercapacitors. It was found that the optimum hydrogel electrolytes prepared with 15 wt.% acrylamide/*N*, *N*′-methylene bisacrylamide possessed the tensile strength and break elongation as high as 18.7 kPa and 743.3%, respectively. The supercapacitors originating from the above electrolytes showed the excellent electrochemical performance. The specific capacitance could achieve 163.7 F g^{-1} at 1.0 A g^{-1} and the corresponding capacitance retention was 87.9% after the constant charge–discharge cycles for 8000 times. Moreover, the supercapacitors could be operated at various bending angles (0°– 180°) and low temperature (− 30 °C) without significant loss of capacitance. These results indicate that the cellulose-based hydrogel electrolytes presented here would have great potential in the application of flexible energy storage devices.

Handling Editor: Stephen Eichhorn.

Address correspondence to E-mail: jingyd@hunnu.edu.cn; zhangxm@hunnu.edu.cn; yuningya@hotmail.com

https://doi.org/10.1007/s10853-022-08112-9

Introduction

The emergence of modern electronics, such as wearable energy devices and soft robots, has put forward higher demands for electrolytes; in this context, the development of "soft" electrolytes with high flexibility, stretch compression capability, and ionic conductivity has attracted great research interest [1]. Hydrogels, being three-dimensional crosslinked hydrophilic networks, have good stretch compression capability and flexibility; more importantly, the water in hydrogels can dissolve various ions. Thus, hydrogels appear to be very suitable materials to make "soft" electrolytes with high electrochemical performance. Indeed, hydrogel electrolytes based on polyvinyl alcohol (PVA) [2], polyacrylamide (PAM) [3], and polyethylene glycol (PEG) [4], have been reported to exhibit good ionic conductivity, flexibility, and mechanical properties. It should be noted that with respect to the growing demands for the environmentally benign and sustainable energy storage, it is still highly desirable to develop hydrogel electrolytes based on natural polymers.

Cellulose is one of the most abundant, renewable, and biodegradable natural biopolymers on earth [5]. Owing to strong intermolecular hydrogen bonds, pristine cellulose is insoluble in water and, as a consequence, not suitable for fabricating hydrogel electrolytes [6]. Chemical modifications associated with weakening intermolecular interaction of cellulose chains can increase the compatibility of cellulose with water greatly [7]; thus, some cellulose derivatives have invoked to prepare hydrogel electrolytes. Wei et al. used carboxymethyl cellulose (CMC) as substrate and methacrylamide propyl trimethyl ammonium chloride (MAPTAC) as annexing agent to fabricate hydrogel electrolytes [8]. The "molecular cages" resulted from the reaction of MAPTAC with carboxylate moieties in CMC could capture Li_2SO_4, and the ultimately derived supercapacitors showed excellent electrochemical performance (174.9 F g^{-1} at 1 A g^{-1}) under high operating voltage (2.1 V). Saborio et al. fabricated so-called all-CMC hydrogel-based supercapacitors with CMC hydrogels as electrodes and NaCl-CMC hydrogels as electrolytes [9]. The resultant supercapacitors showed low specific capacitance of 1.2 mF g^{-1} at an operating voltage of 0.8 V. Also, other cellulose derivatives, such as cellulose nanocrystal (CNC), cellulose nanofiber (CNF), and bacterial cellulose (BC) have been employed to fabricate polymer-based hydrogel electrolytes [10]; however, the above cellulose derivatives are just used as filler agents for enhancing the mechanical properties of the hydrogel electrolytes due to their distinctive nanofibrous structure.

Although considerable progress has been achieved in fabricating hydrogel electrolytes by utilizing cellulose derivatives, the corresponding treatment processes of pristine cellulose are complicated and tedious. Most of the solvents for treating pristine cellulose are multi-component systems containing organic solvents [11], inorganic salts [12], or ionic liquids [13], which would lead to the questions associated with high cost and environmental pollution in large-scale preparation of cellulose-based hydrogel electrolytes. The discovery of aqueous alkali/urea systems for dissolving pristine cellulose opens up a new direction toward convenient fabrication of hydrogel electrolytes based on pristine cellulose. Using epichlorohydrin (ECH) as crosslinking agent, Wang et al. prepared all-solid supercapacitors originating from NaOH/urea-dissolved cellulose solution although the resultant supercapacitors showed low specific capacitance and energy density and the corresponding cellulose-based hydrogel electrolytes possessed low break elongation of ~ 50% [14]. The mechanical properties of cellulose-based hydrogels can be strengthened via the formation of dual-network structured polyacrylamide(PAM)/cellulose hydrogels by dipping the ECH-crosslinked cellulose-based hydrogels into aqueous acrylamide (AM) solution [15]. In this context, dual-network structured β-cyclodextrin/cellulose [16] and PAM/cellulose [17] hydrogels have been immersed in aqueous aniline (ANI)/HCl solution to fabricate cellulose-based hydrogel electrolytes. The resultant polyaniline (PANI)/PAM/cellulose electrolytes showed good break elongation of 680%, and the corresponding stress was 27.3 kPa [17]. Moreover, the derived supercapacitors with carbon cloth as electrodes possessed area-specific capacitance of 835 mF cm^{-2} and capacitance retention of 96% after the constant charge–discharge cycles for 5000 times.

As stated above, aqueous alkali/urea dissolving systems and dual-network structured strategy endow cellulose-based hydrogel electrolytes with good mechanical and electrochemical properties; however, multi-step fabrication methodology and low cellulose

content would limit the application range of such composite hydrogel electrolytes. In this work, AM, ammonium persulfate (APS, as initiating agent), and *N*, *N*-methylene bisacrylamide (MBA, as crosslinking agent) were directly added into NaOH/urea-dissolved cellulose solution. The resultant mixed solution could self-polymerize at ambient temperature, giving rise to PAM/cellulose hydrogel electrolytes with good mechanical and electrochemical properties. Unlike the reported dual-network structured hydrogel electrolytes [16, 17], the sodium hydroxide, used to dissolve pristine cellulose, was directly utilized as conductive species in our PAM/cellulose hydrogel electrolytes fabricated via a simple one-pot process, which omitted the traditional processes of immersing conductive species and reduced the risk of environmental pollution. Moreover, in comparison with the reported dual-network structured cellulose-based hydrogel electrolytes [15–17], the contents of cellulose in our composite hydrogel electrolytes were much higher (∼ 85 wt.%), which indicated the composite electrolytes presented here possessed relatively high greenness. More importantly, quasi solid-state supercapacitors could conveniently obtained via in situ self-polymerization of the precursor solution in the presence of electrodes. In such a way, the traditional "sandwich assembly" could been omitted and, consequently, the interface contact resistance could be reduced, which would be conducive to ultimate electrochemical performance.

Experimental

Materials

Cotton linter (DP ∼ 1400) was purchased from Xuzhou Lierkang Sanitary Material company (Xuzhou, China). Acrylamide (AM, C_3H_5NO, 98%, AR) was purchased by Aladdin Reagent (Shanghai, China). Ammonia persulfate (APS, $(NH_4)_2S_2O_8$, 99%, AR), polytetrafluoroethylene (PTFE, 60 wt%, AR) dispersions, sodium hydroxide (NaOH, 96%, AR), urea ($CO(NH_2)_2$, 99%, AR), *N*, *N*′-methylene bisacrylamide (MBA, $C_7H_{10}N_2O_2$, 98%, AR), ethanol absolute (99.7%, AR), and epichlorohydrin (ECH, C_3H_5ClO, 99%, AR) were purchased from Sinopharm Chemical reagent Co., Ltd (Shanghai, China). Activated carbon (AC: XFP01, specific surface areas of 1800 ± 100 m^2/g, pore sizes of 2.0–2.2 nm, pore volumes of 1.0–1.2 cm^3/g) was purchased from Xianfeng Nano Technology Co.,Ltd (Nanjing, China). Acetylene black (AB, specific surface area of 61 m^2/g, pore size of 12 nm) was purchased from Taiyuan Liziyuan Technology Co.,Ltd (Shanxi, China). Nickel foam (porosity of 97.2%, pore size of 0.1 mm, apparent density of 350 g/m^3) was purchased from Anno New Energy Technology Co., Ltd (Tianjin, China). All regents are used directly without further purification.

Preparation of cellulose-based hydrogel electrolytes

Aqueous cellulose solution (∼ 2.5 wt%) was prepared according to the method reported previously [18]. 7.00 g of NaOH and 12.00 g of urea were dissolved in 100.0 mL of deionized water and the resultant solution was precooled at – 15 °C, followed by adding 2.57 g of cotton linter and stirring extensively for 5 min. The mixture was centrifuged to remove trace amount of solid, leading to transparent cellulose solution. The cellulose hydrogel electrolytes were prepared as follows: 3.0 mL of ECH was added to 15.00 g of the above cellulose solution, and the resultant mixture was stirred at 30 °C for 1 h. After the removal of air bubbles, the homogeneous solution was poured into a petri dish (9 cm). The transparent cellulose hydrogel electrolytes were formed after the chemical crosslinking for 2 h and denoted as $C/PAM_{0\%}$. As for preparing composite cellulose-based hydrogel electrolytes, 2.30 (1.56, 3.03, or 3.75) g of AM, 0.0090 (0.0050, 0.0105, or 0.0130) g of MBA, and 0.150 (0.094, 0.180, or 0.225) g of APS were added into 12.60 (13.43, 12.01, or 11.25) g of the above cellulose solution. After being stirred at 30 °C for 40 min and successive removal of air bubbles, the resultant mixed solution was poured into a petri dish (9 cm). Composite cellulose-based hydrogel electrolytes were formed after the chemical crosslinking for 2 h and denoted as $C/PAM_{15\%}$ ($C/PAM_{10\%}$, $C/PAM_{20\%}$, or $C/PAM_{25\%}$).

Fabrication of quasi solid-state supercapacitors

The working electrodes were prepared by using a modified method reported previously [19]: 0.025 g of AC, 0.003 g of AB, and 0.03 g of aqueous PTFE solution (10%, vol.) were added into 2.0 mL of absolute ethanol to produce homogeneous slurry. The resultant slurry was coated on the nickel foam (1 × 2 cm) with an area of 1 cm^2. Finally, AC

electrodes were obtained by pressing the nickel foam under 10 MPa after being dried at 80 °C for 12 h; meanwhile, the loading mass of each electrode was ~ 2.5 mg. Quasi solid-state supercapacitors were fabricated according to the method reported previously [14]. Typically, the above two AC electrodes were immersed into the desirable uncrosslinked electrolyte solution in a glass mold (1 × 0.5 × 4 cm) and successively, spontaneous chemical crosslinking at room temperature for 2 h gave rise to the quasi solid-state supercapacitors (see Fig. 1). The quasi solid-state supercapacitors based on C/$PAM_{0\%}$, C/$PAM_{10\%}$, C/$PAM_{15\%}$, C/$PAM_{20\%}$, and C/$PAM_{25\%}$ were denoted as SC_0, SC_{10}, SC_{15}, SC_{20}, and SC_{25}, respectively. For comparison purpose, aqueous NaOH solution (1.75 M, being the concentration of NaOH in the cellulose solution) was used as liquid electrolyte to fabricate supercapacitors according to the above processes.

Characterizations

Fourier transformation infrared (FTIR) spectra were obtained on an AV ATAR 370 Thermo Nicolet spectrometer with resolution of 4 cm^{-1}. The samples were subjected to freeze drying and mixed with KBr prior to being pressed into pellets. Powder X-ray diffraction (XRD) patterns were recorded on a Rigaku Ultima IV diffractometer using CuKα radiation (λ = 0.154 nm). Scanning electron microscopy (SEM) images were obtained on a TESCAN MIRA LMS microscope. Before observation, the samples were fractured in liquid nitrogen and sputtered with gold. The mechanical properties of the samples were assessed by a micro-controlled electronic universal testing machine (200 N), and the stretching tests were conducted at a speed of 10 mm/min. Differential scanning calorimetry (DSC) analyses were performed in a NETZSCH DSC200F3 calorimeter.

Electrochemical measurements

The measurement of the resistance of the quasi solid-state supercapacitors was carried out by electrochemical impedance spectroscopy (EIS) using an electrochemical workstation (CHI instrument, Shanghai, China) at the frequency range from 0.01 Hz to 100 kHz. Consequently, the ionic conductivity (σ) could be calculated based on the following equation:

$$\sigma = \frac{L}{S \times R_{es}} \quad (1)$$

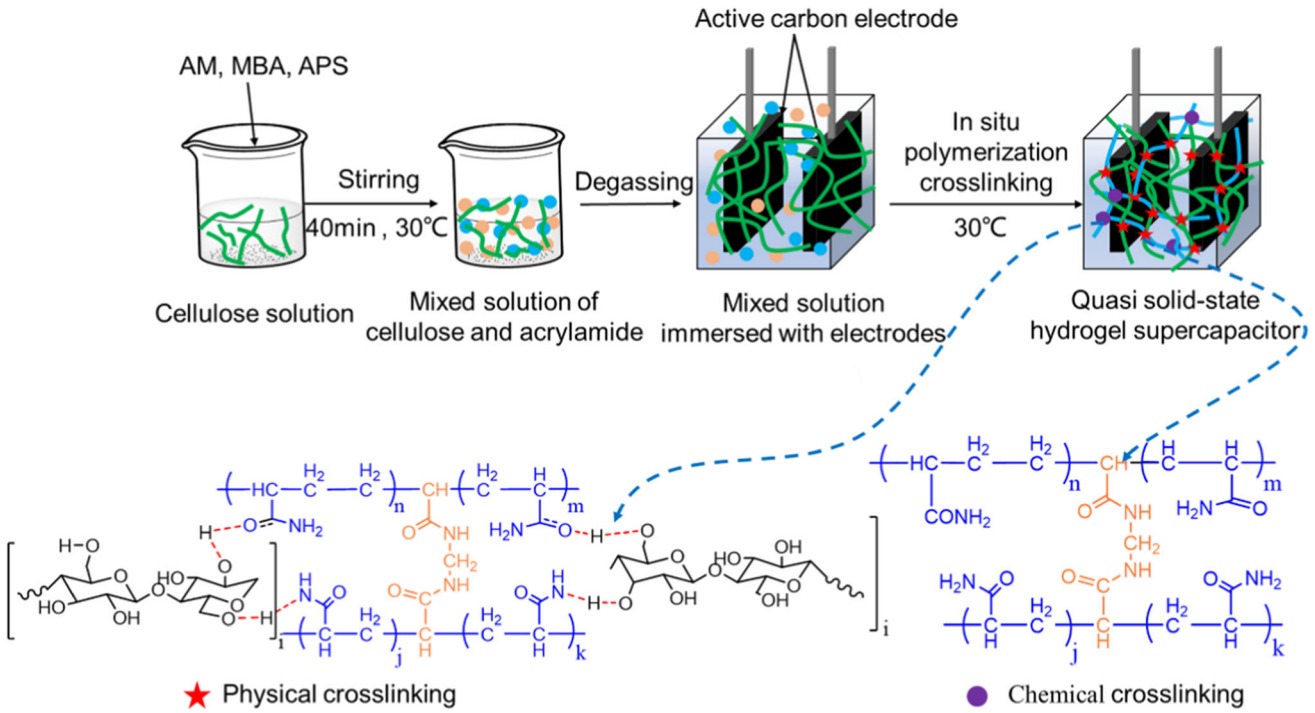

Figure 1 Illustration of the preparation procedure of the cellulose-based hydrogel electrolytes and the corresponding quasi solid-state supercapacitors, together with the interaction in the composite hydrogel networks.

where L is the thickness of the electrolytes (0.5 cm), S is the electrode area (1 cm^2), and R_{es} is the bulk resistance of the electrolytes obtained from the intersection of the curve at the real part in the EIS impedance data.

Cyclic voltammetry (CV) was conducted at different scan rates in order to determine the electrochemical stability of supercapacitors. Galvanostatic charge–discharge (GCD) tests at various current densities and EIS measurements were used to evaluate the electrochemical properties of supercapacitors. The specific capacitance of supercapacitors (C, F g^{-1}), the specific capacitance of electrodes (C_m, F g^{-1}), energy density (E, Wh kg^{-1}), and power density (P, W kg^{-1}) of supercapacitors could be calculated from the GCD curves as follows [20]:

$$C = \frac{I \times \Delta t}{\Delta V \times m} \tag{2}$$

$$C_m = 4 \times C \tag{3}$$

$$E = \frac{1}{8} \times C_m \times \Delta V^2 \times \frac{1000}{3600} \tag{4}$$

$$P = \frac{E}{\Delta t} \times 3600 \tag{5}$$

where I is the discharging current, Δt is the discharging time, and ΔV is the voltage range during the discharging time after internal resistance drop, m is the mass of active electrode materials (AC) on both electrodes. All electrochemical measurements of supercapacitors were measured using a two-electrode system.

Results and discussion

The fabrication route to the cellulose-based hydrogel electrolytes and the corresponding quasi solid-state supercapacitors, together with the interaction in the composite hydrogel networks, is illustrated in Fig. 1. AM (monomer), MBA (crosslinking agent), and APS (initiating agent) were added into the NaOH/urea-dissolved cellulose solution, followed by stirring at 30 °C for 40 min, then spontaneous crosslinking within 2 h led to the composite cellulose-based hydrogel electrolytes. It was proposed that there existed a dual-network structure in the composite electrolytes [15], wherein MBA-crosslinked PAM chains (chemical crosslinking) interlaced with the cellulose chains through H-bonds (physical crosslinking), which would endow the composite electrolytes with good mechanical properties (vide infra). It should be noted that the fabrication processes of supercapacitors could be integrated with the preparation of the composite electrolytes. As shown in Fig. 1, quasi solid-state supercapacitors could conveniently be fabricated by immersing two AC electrodes into the precursor solution used to prepare the composite electrolytes. As such, the traditional "sandwich assembly" could been omitted, which simplified the fabrication processes greatly.

Owing to the fact that the sample of C/$PAM_{0\%}$ composed of cellulose hydrogel could not complete the test under a workload of 200 N, the mechanical properties of the samples of C/$PAM_{x\%}$ containing dual-network structured PAM/cellulose were measured and the relevant results are shown in Fig. 2a. Clearly, the tensile strength of the cellulose-based hydrogel electrolytes gradually increased with increasing the content of AM/MBA in the precursor solution; meanwhile, the corresponding break elongation reached maxima at the content of AM/MBA being 15 wt.%. Although high contents of AM/MBA led to good tensile strength, the elevated crosslinking levels, originated from the increased amount of PAM moieties in the composite hydrogels, were detrimental to the flexibility of the cellulose-based hydrogel electrolytes [21]. Also, high crosslinking level resulted in the inferior ionic conductivities, due to the fact that high crosslinking level would hinder ion transport in the composite hydrogel networks. As shown in Fig. 2b, as the content of AM/MBA increased from 10 wt.% to 25 wt.%, the ionic conductivity of the obtained composite electrolytes decreased from 0.280 to 0.048 S cm^{-1}, although the lowest ionic conductivity observed for C/$PAM_{25\%}$ was higher than the results reported in the literature [22–24]. Nevertheless, the sample of C/$PAM_{15\%}$ possessed a break elongation of 743.3% with the tensile strength being 18.7 kPa (see Fig. 2a'), which is comparable to the composite PAM/cellulose hydrogel electrolytes prepared via the two-step methodology [15].

SEM observations were invoked to verify the textural evolution of the cellulose-based hydrogel electrolytes as the content of AM/MBA in the precursor solution increased. As shown in Fig. 2c, C/$PAM_{0\%}$ composed of cellulose hydrogel had coarse texture with rather thin channel walls, as a consequence, this sample possessed too poor mechanical properties to complete the test of stretching stress–strain. With increasing the content of AM/MBA, the number of

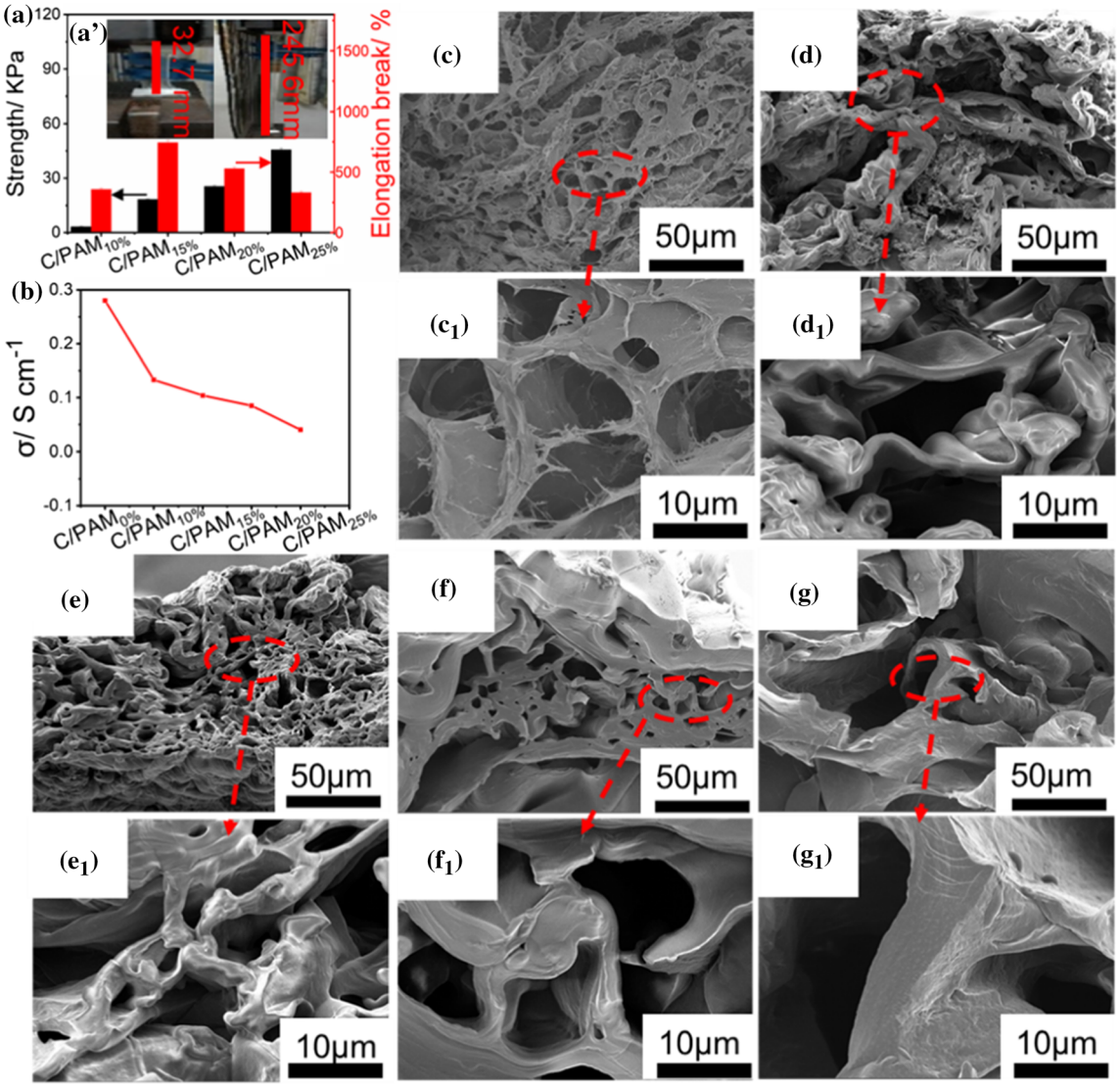

Figure 2 **a** Stretching stress–strain of C/PAM$_{x\%}$ with various contents of AM/MBA. **a′** Optical image of stretching C/PAM$_{15\%}$. **b** Ionic conductivities of C/PAM$_{x\%}$. SEM images of freeze-dried **c-c$_1$** C/PAM$_{0\%}$, **d-d$_1$** C/PAM$_{10\%}$, (**e-e$_1$**) C/PAM$_{15\%}$, **f-f$_1$** C/PAM$_{20\%}$, and **g-g$_1$** C/PAM$_{25\%}$.

pores in the composite electrolytes decreased and the thickness of channel walls increased (see Fig. 2d-d$_1$–g-g$_1$), because the increased amount of PAM moieties in the composite hydrogels led to the elevated crosslinking level [15]. On the other hand, the decreased number of pores and increased thickness of channel walls would, in turn, reduce the ionic conductivity of the composite electrolytes. In this context, the textural evolution in SEM observations can explain the variation trends in the tests of stretching stress–strain and ionic conductivity for the samples of C/PAM$_{x\%}$ very well.

Figure 3 exhibits FTIR spectra and XRD patterns of the pristine cellulose originating from freeze-dried NaOH/urea-dissolved cotton linter, PAM originating from freeze-dried AM-MBA-APS hydrogel, and freeze-dried C/PAM$_{15\%}$ composite hydrogel electrolyte. As shown in Fig. 3a, the pristine cellulose displayed typical stretching vibration of O–H at 3411 cm^{-1}, symmetric stretching vibration of C–H at 2906 cm^{-1}, and bending vibration of H–O–H of the absorbed water at 1643 cm^{-1} [25]. The characteristic vibration bands at 3417, 3195, 1667, and 1112 cm^{-1} could be observed for the sample of PAM, which can be assigned to free -NH$_2$ moieties, associated -NH$_2$

moieties, C=O stretching vibration, and C–N stretching vibration, respectively [26]. No new vibration bands were observed for the sample of $C/PAM_{15\%}$, which indicates that there is not chemical interaction between cellulose and PAM chains. However, obvious shifts of vibration bands, that is, the stretching vibration of O–H at 3411 cm^{-1} in the pristine cellulose shifting to 3439 cm^{-1}, vibration band of associated $–NH_2$ moieties at 3195 cm^{-1} in PAM shifting to 3188 cm^{-1}, and the stretching vibration of C–N at 1112 cm^{-1} in PAM shifting to 1120 cm^{-1}, could be observed for $C/PAM_{15\%}$, which suggest that there exists strong H-bond interaction between PAM and cellulose chains [15, 27].

As shown in Fig. 3b, the pristine cellulose exhibited three diffraction peaks at 2θ = 12.2°, 20.1°, and 22.6°, which is the characteristic of cellulose-II obtained at the temperature below − 15 °C [28]. The sample of PAM showed a broad diffraction peak centered at 24.4°, indicating amorphous carbon characteristic of PAM. In the case of $C/PAM_{15\%}$, the characteristic peaks assigned to cellulose-II disappeared and a new broad diffraction peak centered at 21.6° was observed. The vanishment of the characteristic peaks assigned to cellulose-II indicated that PAM chains had inserted into cellulose chains, destroying the crystal structure of cellulose-II while the crosslinking of MBA among PAM chains led to the coexistence of crystalline and amorphous domains in cellulose structure [17]. Therefore, $C/PAM_{15\%}$, showed a broad diffraction peak centered at 21.6°. Combining FTIR and XRD results, it is logical to conclude that PAM chains have been incorporated with cellulose chains in the one-pot methodology presented here, yielding dual-network structured PAM/cellulose hydrogels.

The CV curves of the samples of SC_x measured at 100 mV s^{-1} are shown in Fig. 4a. All the CV curves displayed symmetrical quasi-rectangular shape, implying rapid electrochemical response and ideal double-layer capacitive behavior [29]. Increasing the content of AM/MBA in the precursor solution resulted in the decreased rectangle areas, which can be due to the fact that the decreased number of pores and increased thickness of channel walls at the elevated content of AM/MBA, as observed in SEM, would hinder ion transport and increase internal resistance. This could be further confirmed by EIS spectra. As shown in Fig. 4b, R_{es} of SC_x increased from 1.76 to 12.5 Ω as the content of AM/MBA was elevated from 0 wt% to 25 wt%. It should be noted that irrespective of the content of AM/MBA, all of the Nyquist plots consisted of negligible semicircles in the medium-frequency region (see Fig. 4b inset), which is an indication that all of SC_x presented here possessed very low interfacial charge-transfer resistances. Considering the one-pot methodology for assembling SC_x, it is not surprising to find the above results [30]. Figure 4c displays the GCD curves of the samples of SC_x, and the calculated specific capacitances are shown in Fig. 4d. Owing to the increased R_{es}, the specific capacitance of SC_x decreased with the elevated content of AM/MBA; more specifically, the samples of SC_0, SC_{10}, SC_{15}, SC_{20}, and SC_{25} possessed the specific capacitances of 180.6, 168.0, 163.7, 130.1, and 125.7 F g^{-1} at current density of 1 A g^{-1}, respectively. Considering good mechanical properties and relatively high specific capacitance, the sample of SC_{15} based on $C/PAM_{15\%}$ was chosen for further electrochemical tests.

The CV curves of SC_{15} at various scan rates are shown in Fig. 5a. The CV curve of SC_{15} displayed a

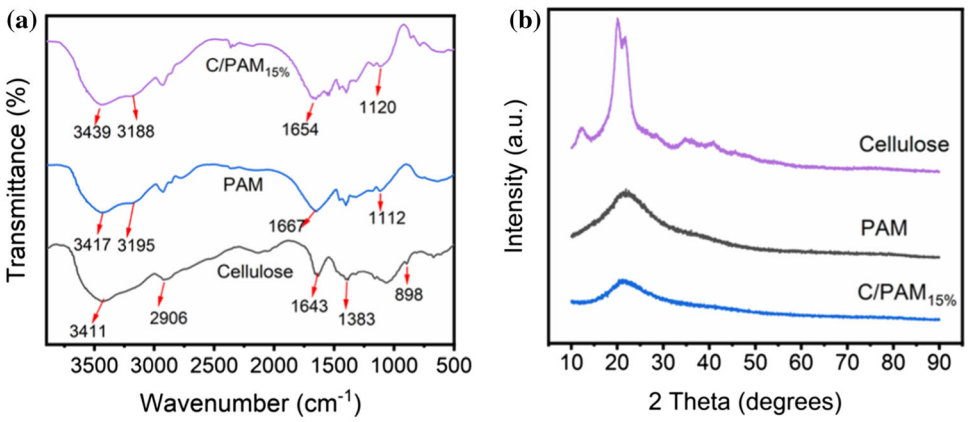

Figure 3 **a** FTIR and **b** XRD of pristine cellulose, PAM, and $C/PAM_{15\%}$.

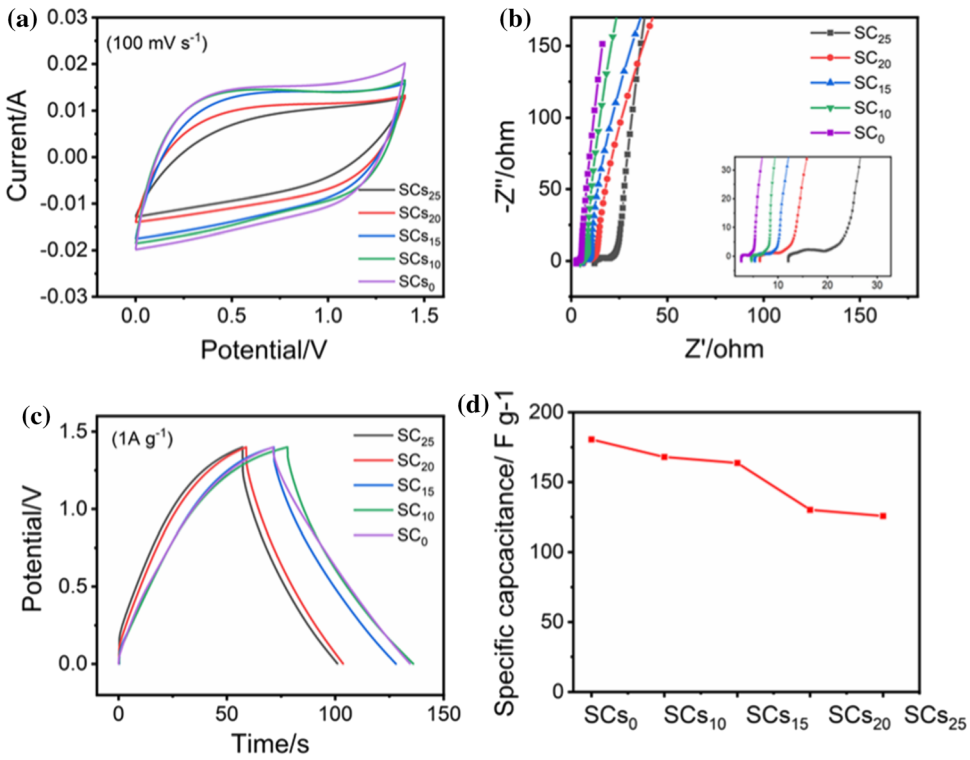

Figure 4 **a** CV curves of SC_x measured at 100 mV s^{-1}. **b** The Nyquist plots with the enlarged medium-frequency range in the inset. **c** The GCD curves of SC_x at 1 A g^{-1}. **d** The calculated specific capacitances of SC_x at 1 A g^{-1}.

symmetrical shape even at a scan rate as high as 200 mV s^{-1}, which indicates that the sample possesses low charge transfer resistance and excellent capacitive behavior [31]. Figure 5b exhibits the GCD curves of SC_{15} at various current densities ranging from 0.5 to 7.5 A g^{-1}. Triangle-shaped curves could been observed at all current densities measured, which suggests that SC_{15} has perfect double-layer capacitive behavior and low internal resistance. The sample of SC_{15} showed a specific capacitance of 163.7 F g^{-1} at current density being 1.0 A g^{-1}, which is significantly higher than most of the supercapacitors with AC as electrodes (see Table 1). Figure 5c represents the capacitance retention and Coulombic efficiency of SC_{15} during constant charge–discharge cycles at 7.5 A g^{-1} for 8000 times. It should be noted that the initial specific capacitance of SC_{15} was 95.7 F g^{-1} at high current density, still superior to the cellulose-based supercapacitors tested at the same current density [32]. After constant charge–discharge cycles at 7.5 A g^{-1} for 4000, 5000, and 8000 times, the capacitance retention rates of SC_{15} were 91.8%, 90.9%, and 87.9%, respectively, while the corresponding Coulombic efficiencies remained at 99.3%, 99.0%, and 97.4%, respectively. The above results indicate the supercapacitors fabricated with the cellulose-based hydrogel electrolytes of $C/PAM_{15\%}$ possess outstanding electrochemical stability. For comparison purpose, the supercapacitors fabricated with the cellulose hydrogel electrolytes of $C/PAM_{0\%}$ or the liquid electrolytes (1.75 M NaOH) were subjected to the same stability tests, and the results are shown in Figs. S1, S2, respectively. The sample of SC_0 based on the cellulose hydrogel electrolytes showed a capacitance retention rate of 82.9% after 5000 cycles, which is much lower than that of SC_{15} based on the cellulose-based composite hydrogel electrolytes (90.9%). Likewise, the sample based on the liquid electrolytes displayed inferior electrochemical stability to SC_{15}, and a capacitance retention rate of 80.2% was observed after only 4000 cycles. As for hydrogel electrolytes, free water could decompose into OH^-/H^+ ions at high potential [33] and the volatilization of free water could occur during the time-consuming tests, thus, the water retention capacity of electrolytes would play a crucial role in the electrochemical stability of the supercapacitors. It was reported that PAM possessed higher water retention capacity than cellulose [34], in this context, it is not surprising to find the decreasing electrochemical stability in the following order $SC_{15} > SC_0 >$ the supercapacitors based on the liquid electrolytes (1.75 M NaOH). Furthermore, the sample of SC_{15} had an energy density of 12.5 Wh kg^{-1} at a power density of

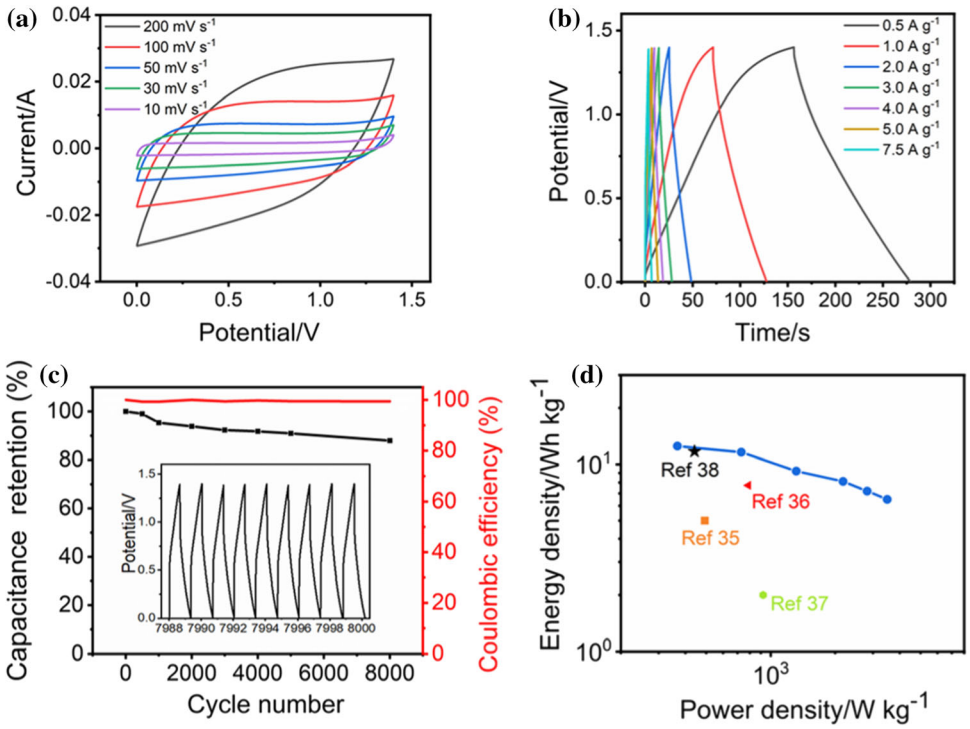

Figure 5 **a** CV curves of SC_{15} measured at various scan rates. **b** The GCD curves of SC_{15} at various current densities. **c** Capacitance retention and Coulombic efficiency of SC_{15} during constant charge–discharge cycles (7.5 A g^{-1}), the inset is the GCD curves of the last 12 cycles of 8000 cycles. **d** Ragone plot of SC_{15} compared to the reported results.

Table 1 Comparison of SC_{15} with previously reported supercapacitors

Electrode	Electrolyte	Voltage (V)	Capacitance (F g^{-1})	Ref
AC	MCM-H	0–1.5	91.8 (1.0 A g^{-1})	[36]
AC	AA/$CaCl_2$	0–1.0	144.6 (0.5 A g^{-1})	[39]
AC	PEG/H_3PO_4	0–1.0	64.0 (2.0 mV s^{-1})	[37]
AC	LC-GPE	0–1.0	120.0 (1.0 A g^{-1})	[40]
AC	C/PVA/KOH	0–1.6	160.0 (0.5 A g^{-1})	[33]
AC	B-PVA/KCl/GO	0–1.0	156.0 (0.3 A g^{-1})	[35]
AC	pPBI-IL	0–1.0	110.0 (1.0 A g^{-1})	[41]
AC	PVA-g-TMAC/KCl	0–1.0	85.4 (1.0 A g^{-1})	[42]
AC	PAMBGCo	− 1.0–1.0	130.0 (0.3 A g^{-1})	[43]
AC	Li-AG/PAM	0–0.8	84.7 (0.2 A g^{-1})	[44]
AC	C/PVA/H_2SO_4	0–1.0	112.0 (1.0 A g^{-1})	[45]
AC	$C/PAM_{15\%}$	0–1.4	163.7 (1.0 A g^{-1})	This work

354.2 W kg^{-1} (see Fig. 5d), superior to most of the supercapacitors based on hydrogel electrolytes [35–38].

Considering the facts that hydrogel electrolytes could lose elasticity and/or conductivity at subzero temperatures and dehydrate at high temperatures and that a good temperature resistance would be important in practical applications, the electrochemical properties of SC_{15} were further investigated at the temperatures ranging from – 30 °C to 80 °C. As shown in Fig. 6a, b, both the CV and GCD curves of SC_{15} tested at 80 °C almost overlapped with the corresponding curves at 30 °C and the ionic conductivity was 0.100 S/cm (see Fig. 6c), slightly higher than that at 30 °C (0.091 S/cm). The calculated specific capacitance at 80 °C was 155.3 F g^{-1}, being 95.7% of the initial value at 30 °C (163.7 F g^{-1}). The above results indicate the sample of SC_{15} has a good resistance against high temperatures. In contrast, because of the significantly decreasing ionic conductivity (0.022 S/cm), the CV curve of SC_{15} at − 30 °C offset from rectangular shape slightly although the GCD curve remained triangular shape. As a consequence, the calculated specific capacitance at − 30 °C was 130.8 F g^{-1}. Although the declined electrochemical properties were observed for SC_{15} at

− 30 °C, the ionic conductivity, specific capacitance, and the corresponding capacitance retention (80.2%) could bear comparison with the reported results [46], which indicates that the composite cellulose-based hydrogel electrolytes presented here possess good anti-freezing performance. In order to verify the superiority of the composite hydrogel electrolytes, DSC was used to analyze the anti-freezing performances of the samples of $C/PAM_{0\%}$ and $C/PAM_{15\%}$. As shown in Fig. 6d, the sample of $C/PAM_{0\%}$ showed a clear exothermic peak centered at − 32 °C, which can be assigned to the freezing point of NaOH hydrates [47], whereas no exothermic peak could be observed for $C/PAM_{15\%}$. Based on these results, it was proposed that the dual-network structured $C/PAM_{15\%}$ possesses stronger affinity to NaOH hydrates, in comparison with $C/PAM_{0\%}$ consisting of the single network structured cellulose, which inhibits the crystallization of NaOH hydrates and, consequently, endows the composite hydrogel electrolytes with higher anti-freezing performance (see Fig. 6d).

To further illustrate the flexibility of the composite hydrogel electrolytes, the electrochemical performance of SC_{15} was studied under various bending states. As shown in Fig. 7a, b, there were no noticeable changes in the CV and GCD curves after SC_{15} was bent at various angles, indicating the supercapacitors possess good flexibility. The optical images of SC_{15} at various bending angles (from 0° to 180°) are shown in Fig. 7c. No peeling phenomenon between the electrodes and electrolytes could be observed for the sample of SC_{15} at any bending angle tested, which suggests that the supercapacitors presented here have excellent stability and flexibility, possibly originated from the one-pot assembling methodology. In addition, the ability of energy storage of SC_{15} in the actual situation was demonstrated. As shown in Fig. 7d, after the single SC_{15} was charged for a while,

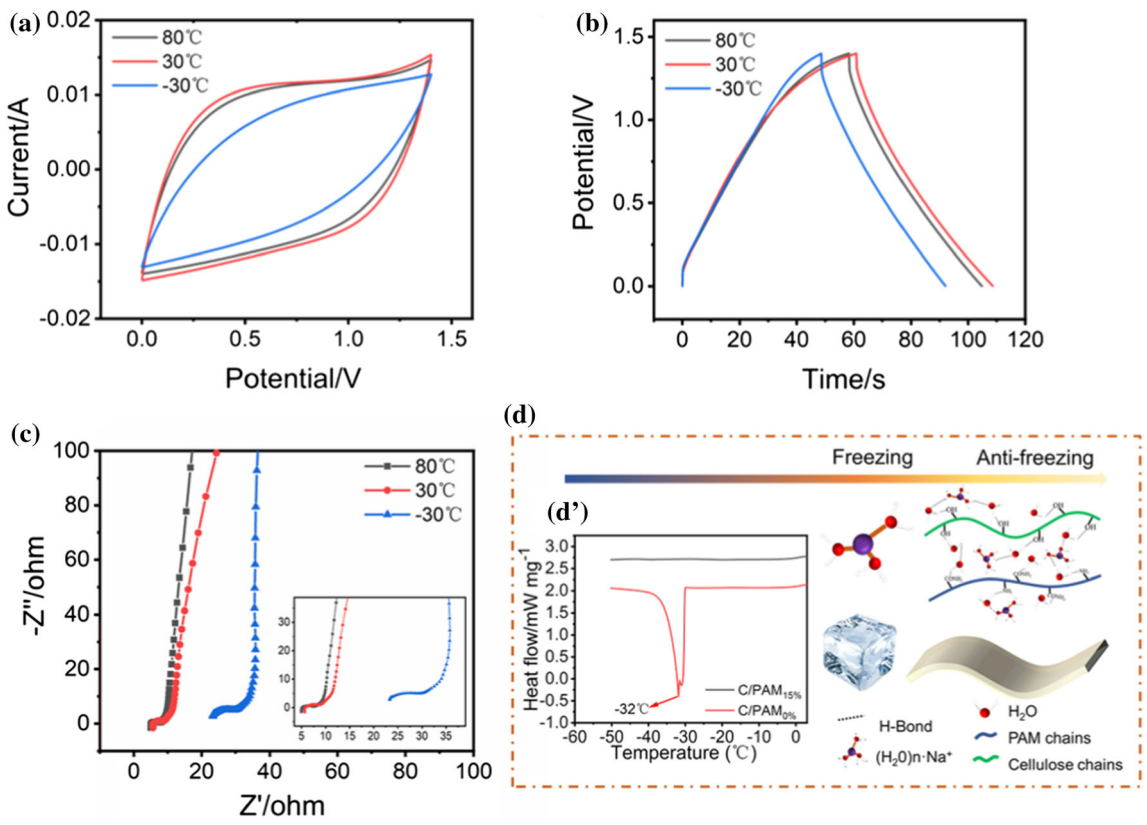

Figure 6 **a** CV and **b** GCD curves of SC_{15} at various temperatures. **c** The Nyquist plots of SC_{15} at various temperatures. **d** Anti-freezing mechanism diagram of $C/PAM_{15\%}$ composite hydrogel electrolytes, **d′** DSC profiles of $C/PAM_{0\%}$ and $C/PAM_{15\%}$ composite hydrogel electrolytes.

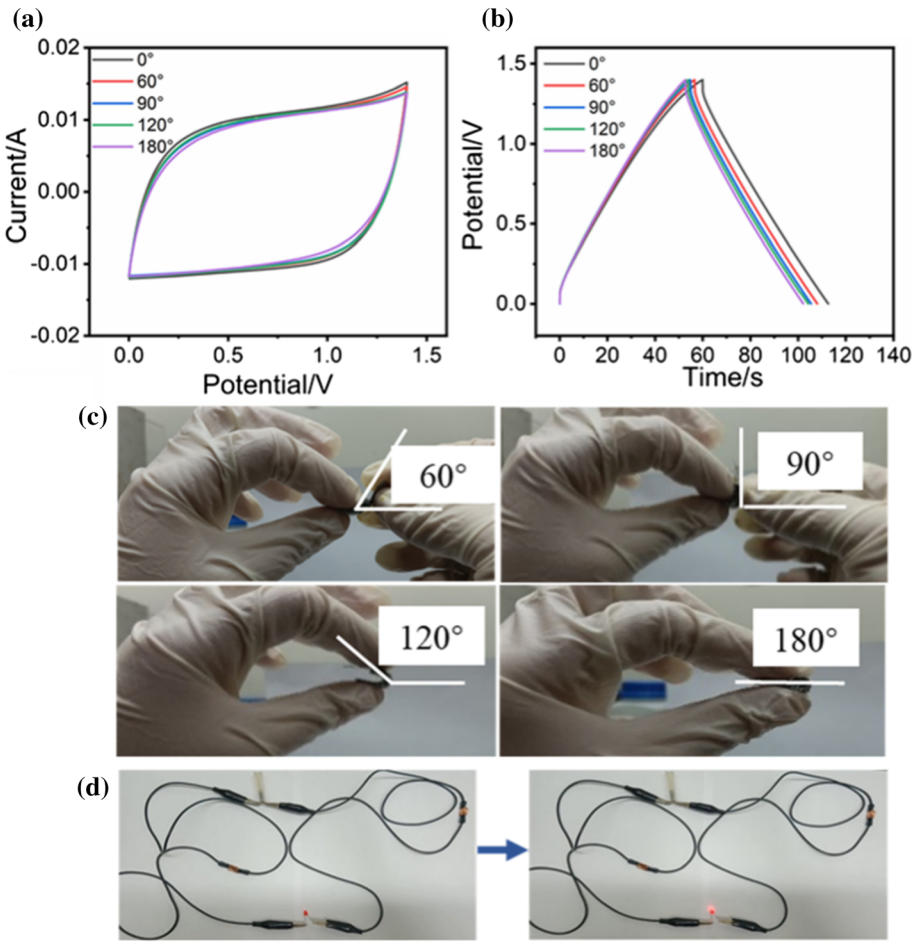

Figure 7 **a** CV and **b** GCD curves of SC_{15} at various bending angles. **c** The optical images of flexible SC_{15} at various bending angles. **d** Lighting a red LED bulb by the charged single SC_{15}.

it could light a red light-emitting diode (LED) bulb easily.

Conclusions

Herein, AM, APS as initiating agent, and MBA as crosslinking agent were directly added into NaOH/urea-dissolved cellulose solution, followed by self-polymerization at ambient temperature, PAM/cellulose hydrogel electrolytes with good mechanical and electrochemical properties were obtained. As such, the sodium hydroxide, used to dissolve pristine cellulose, could be directly utilized as conductive species. Quasi solid-state supercapacitors could conveniently obtained via in situ self-polymerization of the above precursor solution in the presence of AC electrodes without the traditional "sandwich assembly" processes. The resultant supercapacitors exhibited high specific capacitance of 163.7 F g^{-1} at 1.0 A g^{-1}, energy density of 12.5 Wh kg^{-1} at power density of 354.2 W kg^{-1}, and capacitance retention of 87.9% after the constant charge–discharge cycles for 8000 times. Furthermore, the electrochemical performance of the supercapacitors did not deteriorate significantly at − 30 °C or after being bent at angles of 0–180°. The above results, together with high content of cellulose (∼ 85%) in the composite hydrogel electrolytes, indicated that the cellulose-based hydrogel electrolytes and the corresponding quasi solid-state supercapacitors presented here would be potential candidates in the application of flexible energy storage devices.

Acknowledgements

This study was funded by the Large-scale instrument opening fund of Hunan Normal University (21CSZ076), the Key fund of Hunan Educational Committee, China, for financial support (18B025), and Changsha Natural Foundation of Hunan

Provincial, China (kq2202245). N. Yu is grateful to the financial support from Guangzhou Lingwe Technology Co., Ltd.

Declarations

Conflict of interest The authors declare that they have no conflict of interest.

Supplementary Information: The online version contains supplementary material available at https://doi.org/10.1007/s10853-022-08112-9.

References

[1] KS Oh JH Kim SH Kim 2021 Single-ion conducting soft electrolytes for semi-solid lithium metal batteries enabling cell fabrication and operation under ambient conditions Adv Energy Mater 11 2101813 https://doi.org/10.1002/aenm.202101813

[2] XJ Gao QZ Hu KJ Sun 2021 A novel all-in-one integrated flexible supercapacitor based on self-healing hydrogel electrolyte J Alloys Compd 888 161554 https://doi.org/10.1016/j.jallcom.2021.161554

[3] NS Rafidi M Hina S Gunalan 2022 Renewable and soft dynamic supercapacitors based on poly (acrylamide) hydrogel electrolytes and porous carbon electrodes Polym Bull 79 1 18 https://doi.org/10.1007/s00289-021-04032-x

[4] S Ishii H Kokubo K Hashimoto 2017 Tetra-PEG network containing ionic liquid synthesized via Michael addition reaction and its application to polymer actuator Macromolecules 50 2906 2915 https://doi.org/10.1021/acs.macromol.6b02750

[5] DW Zhao CJ Chen Q Zhang 2017 High performance, flexible, solid-state supercapacitors based on a renewable and biodegradable mesoporous cellulose membrane Adv Energy Mater 7 1700739 https://doi.org/10.1002/aenm.201700739

[6] XP Shen JL Shamshina P Berton 2016 Hydrogels based on cellulose and chitin: fabrication, properties, and applications Green Chem 18 53 75 https://doi.org/10.1039/c5gc02396c

[7] M Oprea SI Voicu 2020 Recent advances in composites based on cellulose derivatives for biomedical applications Carbohydr Polym 247 116683 https://doi.org/10.1016/j.carbpol.2020.116683

[8] JJ Wei J Zhou SS Su 2018 Water-deactivated polyelectrolyte hydrogel electrolytes for flexible high-voltage supercapacitors Chemsuschem 11 3410 3415 https://doi.org/10.1002/cssc.201801277

[9] MG Saborio P Svelic J Casanovas 2019 Hydrogels for flexible and compressible free standing cellulose supercapacitors Eur Polymer J 118 347 357 https://doi.org/10.1016/j.eurpolymj.2019.06.011

[10] YN Zhang HL Qin M Alfred 2021 Reaction modifier system enable double-network hydrogel electrolyte for flexible zinc-air batteries with tolerance to extreme cold conditions Energy Storage Mater 42 88 96 https://doi.org/10.1016/j.ensm.2021.07.026

[11] ERD Seiler Y Takeoka M Rikukawa 2020 Development of a novel cellulose solvent based on pyrrolidinium hydroxide and reliable solubility analysis RSC Adv 10 11475 11480 https://doi.org/10.1039/d0ra01486a

[12] L Yang L Song Y Feng 2020 Zinc ion trapping in a cellulose hydrogel as a solid electrolyte for a safe and flexible supercapacitor J Mater Chem A 8 12314 12318 https://doi.org/10.1039/d0ta04360e

[13] D Kasprzak E Krystkowiak I Stępniak 2019 Dissolution of cellulose in novel carboxylate-based ionic liquids and dimethyl sulfoxide mixed solvents Eur Polymer J 113 89 97 https://doi.org/10.1016/j.eurpolymj.2019.01.053

[14] HF Wang J Wu J Qiu 2019 In situ formation of a renewable cellulose hydrogel electrolyte for high-performance flexible all-solid-state asymmetric supercapacitors Sustain Energy Fuels 3 3109 3115 https://doi.org/10.1039/c9se00339h

[15] FC Lin XC Lu Z Wang 2018 In situ polymerization approach to cellulose–polyacrylamide interpenetrating network hydrogel with high strength and pH-responsive properties Cellulose 26 1825 1839 https://doi.org/10.1007/s10570-018-2171-y

[16] Q Gong Y Li X Liu 2020 A facile preparation of polyaniline/cellulose hydrogels for all-in-one flexible supercapacitor with remarkable enhanced performance Carbohydr Polym 245 116611 https://doi.org/10.1016/j.carbpol.2020.116611

[17] YQ Li Q Gong XH Liu 2021 Wide temperature-tolerant polyaniline/cellulose/polyacrylamide hydrogels for high-performance supercapacitors and motion sensors Carbohydr Polym 267 118207 https://doi.org/10.1016/j.carbpol.2021.118207

[18] J Cai LN Zhang 2005 Rapid dissolution of cellulose in LiOH/urea and NaOH/urea aqueous solutions Macromol Biosci 5 539 548 https://doi.org/10.1002/mabi.200400222

[19] LQ Fan CL Geng YL Wang 2020 Design of a redox-active "water-in-salt" hydrogel polymer electrolyte for superior-performance quasi-solid-state supercapacitors New J Chem 44 17070 17078 https://doi.org/10.1039/d0nj04102e

[20] MX Wang LD Fan G Qin et al 2020 Flexible and low temperature resistant semi-IPN network gel polymer electrolyte membrane and its application in supercapacitor J Membr Sci 597 117740 https://doi.org/10.1016/j.memsci.2019.117740

[21] S Tröger-Müller C Liedel 2019 Sustainable polyimidazolium networks as versatile hydrogel materials ACS Appl Polym Mater 1 2606 2612 https://doi.org/10.1021/acsapm.9b00491

[22] HZ Yang XW Ji YT Tan 2019 Modified supramolecular carboxylated chitosan as hydrogel electrolyte for quasi-solid-state supercapacitors J Power Sources 441 227174 https://doi.org/10.1016/j.jpowsour.2019.227174

[23] DS Silvaraj S Bashir M Hina 2021 Tailorable solid-state supercapacitors based on poly (*N*-hydroxymethylacrylamide) hydrogel electrolytes with high ionic conductivity J Energy Storage 35 102320 https://doi.org/10.1016/j.est.2021.102320

[24] MM Yu XW Ji F Ran 2021 Chemically building interpenetrating polymeric networks of Bi-crosslinked hydrogel macromolecules for membrane supercapacitors Carbohydr Polym 255 117346 https://doi.org/10.1016/j.carbpol.2020.117346

[25] MZ Zhang M Li NY Yu 2021 Fabrication of AgCl@tannic acid-cellulose hydrogels for $NaBH_4$-mediated reduction of 4-nitrophenol Cellulose 28 3515 3529 https://doi.org/10.1007/s10570-021-03721-0

[26] RQ Liu SM Liang XZ Tang 2012 Tough and highly stretchable graphene oxide/polyacrylamide nanocomposite hydrogels J Mater Chem 22 14160 14167 https://doi.org/10.1039/c2jm32541a

[27] TX Zhu Y Cheng CY Cao 2020 A semi-interpenetrating network ionic hydrogel for strain sensing with high sensitivity, large strain range, and stable cycle performance Chem Eng J 385 123912 https://doi.org/10.1016/j.cej.2019.123912

[28] X Chen J Chen T You 2015 Effects of polymorphs on dissolution of cellulose in NaOH/urea aqueous solution Carbohydr Polym 125 85 91 https://doi.org/10.1016/j.carbpol.2015.02.054

[29] JL Shi WC Du YX Yin 2014 Hydrothermal reduction of three-dimensional graphene oxide for binder-free flexible supercapacitors J Mater Chem A 2 10830 10834 https://doi.org/10.1039/c4ta01547a

[30] LF Chen ZH Huang HW Liang 2014 Three-dimensional heteroatom-doped carbon nanofiber networks derived from bacterial cellulose for supercapacitors Adv Func Mater 24 5104 5111 https://doi.org/10.1002/adfm.201400590

[31] KL Aken Van CR Pérez Y Oh 2015 High rate capacitive performance of single-walled carbon nanotube aerogels Nano Energy 15 662 669 https://doi.org/10.1016/j.nanoen.2015.05.028

[32] D Kasprzak I Stepniak M Galinski 2018 Electrodes and hydrogel electrolytes based on cellulose: fabrication and characterization as EDLC components J Solid State Electrochem 22 3035 3047 https://doi.org/10.1007/s10008-018-4015-y

[33] ZX Zhao Y Huang F Qiu 2021 A new environmentally friendly gel polymer electrolyte based on cotton-PVA composited membrane for alkaline supercapacitors with increased operating voltage J Mater Sci 56 11027 11043 https://doi.org/10.1007/s10853-021-05987-y

[34] Y Masahiro M Mitsuhiro S Isao 1992 Porous structure and rheological properties of hydrogels of highly water-absorptive cellulose graft copolymers J Appl Polym Sci 45 805 812

[35] H Peng YY Lv GG Wei 2019 A flexible and self-healing hydrogel electrolyte for smart supercapacitor J Power Sources 431 210 219 https://doi.org/10.1016/j.jpowsour.2019.05.058

[36] ZY Xun SP Ni ZH Gao 2019 Construction of polymer electrolyte based on soybean protein isolate and hydroxyethyl cellulose for a flexible solid-state supercapacitor Polymers (Basel) 11 1895 1912 https://doi.org/10.3390/polym11111895

[37] YN Sudhakar DK Bhat M Selvakumar 2016 Ionic conductivity and dielectric studies of acid doped cellulose acetate propionate solid electrolyte for supercapacitor Polym Eng Sci 56 196 203 https://doi.org/10.1002/pen.24243

[38] HJ Fei N Saha N Kazantseva 2017 A highly flexible supercapacitor based on MnO_2/RGO nanosheets and bacterial cellulose-filled gel electrolyte Materials 10 1251 https://doi.org/10.3390/ma10111251

[39] Y Khan S Bashir M Hina et al 2020 Effect of charge density on the mechanical and electrochemical properties of poly (acrylic acid) hydrogel electrolytes based flexible supercapacitors Mater Today Commun 25 101558 https://doi.org/10.1016/j.mtcomm.2020.101558

[40] F Qiu Y Huang X Hu 2019 An ecofriendly gel polymer electrolyte based on natural lignocellulose with ultrahigh electrolyte uptake and excellent ionic conductivity for alkaline supercapacitors Acs Appl Energy Mater 2 6031 6042 https://doi.org/10.1021/acsaem.9b01150

[41] TJ Mao S Wang X Wang 2019 High-temperature and all-solid-state flexible supercapacitors with excellent long-term stability based on porous polybenzimidazole/functional ionic liquid electrolyte ACS Appl Mater Interfaces 11 17742 17750 https://doi.org/10.1021/acsami.9b00452

[42] ZK Wang QM Pan 2017 An omni-healable supercapacitor integrated in dynamically cross-linked polymer networks Adv Funct Mater 27 1700690 https://doi.org/10.1002/adfm.201700690

[43] ST Gunday T Qahtan E Cevik 2021 Highly flexible and tailorable cobalt-doped cross-linked polyacrylamide-based electrolytes for use in high-performance supercapacitors Chem Asian J 16 1438 1444 https://doi.org/10.1002/asia.202100276

[44] T Lin MN Shi FR Huang 2018 One-pot synthesis of a double-network hydrogel electrolyte with extraordinarily excellent mechanical properties for a highly compressible and bendable flexible supercapacitor ACS Appl Mater Interfaces 10 29684 29693 https://doi.org/10.1021/acsami.8b11377

[45] ZX Zhao Y Huang WH Ren 2021 Natural biomass hydrogel based on cotton fibers/PVA for acid supercapacitors ACS Appl Energy Mater 4 9144 9153 https://doi.org/10.1021/acsaem.1c01404

[46] HQ Wang Z Li M Zuo 2022 Stretchable, freezing-tolerant conductive hydrogel for wearable electronics reinforced by cellulose nanocrystals toward multiple hydrogen bonding Carbohydr Polym 280 119018 https://doi.org/10.1016/j.carbpol.2021.119018

[47] S Wang K Lyu P Sun 2017 Influence of cation on the cellulose dissolution investigated by MD simulation and experiments Cellulose 24 4641 4651 https://doi.org/10.1007/s10570-017-1456-x